On properties of Velikhov-Chandrasekhar MRI in ideal and non-ideal plasma

N. Shakura *, K. Postnov

Sternberg Astronomical Institute, Moscow M.V. Lomonosov State University, Universitetskij pr., 13, 119992, Moscow, Russia

Printed 27 January 2022

Received ... Accepted ...

ABSTRACT

Conditions of Velikhov-Chandrasekhar magneto-rotational instability in ideal and non-ideal plasmas are examined. Linear WKB analysis of hydromagnetic axially symmetric flows shows that in the Rayleigh-unstable hydrodynamic case where the angular momentum decreases with radius, the MRI branch becomes stable, and the magnetic field suppresses the Rayleigh instability at small wavelengths. We investigate the limiting transition from hydro-magnetic flows to hydrodynamic flows. The Rayleigh mode smoothly transits to the hydrodynamic case, while the Velikhov-Chandrasekhar MRI mode completely disappears without the magnetic field. The effects of viscosity and magnetic diffusivity in plasma on the MRI conditions in thin accretion discs are studied. We find the limits on the mean free-path of ions allowing MRI to operate in such discs.

(MN LATEX style file v2.2)

Key words: hydrodynamics, instabilities, magnetic fields

INTRODUCTION

In the end of the 1950s - beginning of the 1960s, E. Velikhov and S. Chandrasekhar studied the stability of sheared hydromagnetic flows (Velikhov 1959; Chandrasekhar 1960). In these papers, the magneto-rotational instability (MRI) in axisymmetric flows with magnetic field was discovered. MRI arises when a relatively small seed poloidal magnetic field is present in the fluid. This instability was applied to astrophysical accretion discs in the influential paper by Balbus & Hawley 1991, and since then has been considered as the major reason for the turbulence arising in accretion discs (see Balbus & Hawley (1998) for a review). Non-linear numerical simulations (e.g. Hawley, Gammie & Balbus 1995; Sorathia et al. 2012; Hawley et al. 2013) confirmed that MRI can sustain turbulence and dynamo in accretion discs. However, semi-analytical and numerical simulations (see, for example, Masada & Sano 2008; Stone 2011; Hawley et al. 2013; Suzuki & Inutsuka 2014; Nauman & Blackman 2015) suggest that the total (Reynolds + Maxwell) stresses due to MRI are insufficient to cause the effective angular momentum transfer in accretion discs in terms of the phenomenological alpha-parameter α_{SS} (Shakura & Sunyaev 1973), giving rather low values $\alpha_{SS} \sim 0.01 - 0.03$. Note that from the observational point of view, the alpha-parameter can be reliably evaluated, e.g., from the analysis of non-stationary accretion discs in X-ray novae (Suleimanov, Lipunova & Shakura 2008), dwarf-nova and AM CVn stars (Kotko & Lasota 2012), and turns out to be an order of magnitude higher than typically found in the numerical MRI simulations.

In this paper we use the local linear analysis of MRI in

the WKB-approximation by Balbus and Hawley (1991) to examine properties of MRI for different laws of differential rotation in weakly magnetized flows, $\Omega^2(r) \propto r^{-n}$, i.e. when the solution to linearized MHD equations in the Boussinesq approximation is searched for in the form ~ $e^{i(\omega t - k_r r - k_z z)}$, where k_r, k_z are wave vectors in the radial and normal direction to the disc plane, respectively, in the cylindrical coordinates.

In this approximation, the dispersion relation represents a biquadratic algebraic equation. The linear local analysis of unstable modes in this case was performed earlier (see, e.g., Balbus (2012)). Here we emphasize the different behaviour of stable and unstable modes of this equation for different rotation laws of the fluid. We show that in the Rayleigh-unstable hydrodynamic case where the angular momentum decreases with radius, the Velikhov-Chandrasekhar MRI does not arise, and the magnetic field suppresses the Rayleigh instability at small wavelengths.

Then we turn to the analysis of non-ideal plasma characterized by non-zero kinematic viscosity ν and magnetic diffusivity η . This problem has been addressed previously by different authors (see, e.g. Balbus & Hawley (1998); Sano & Miyama (1999); Ji, Goodman & Kageyama (2001); Balbus (2004); Islam & Balbus (2005); Pessah & Chan (2008), among others), aimed at studying various aspects of the MRI physics and applications. To keep the paper self-contained, we re-derive the basic dispersion relation in the general case and investigate its behaviour for different values of the magnetic Prandtl number $P_m = \nu/\eta$ and the kinematic vicosity ν . Specifically, we consider the limitations implied by the viscosity in accretion discs with finite thickness, and find phenomenologically interesting constraints on the disc parameters where MRI can operate.

The structure of the paper is as follows. In Section 2 we repeat

the linear WKB analysis for small perturbations in an ideal fluid and consider five different cases for MRI and Rayleigh modes. We also investigate the behaviour of MRI at vanishing magnetic field. In Section 3 we generalize the linear analysis for non-ideal plasma with non-zero viscosity and magnetic diffusion. First we analytically investigate the growth of linear perturbations in a plasma with the Prandtl number $P_m = 1$, and then consider the case of a plasma with arbitrary Prandtl number and viscosity. We discuss the results in Section 4. In Appendix A we delineate the derivation of the dispersion equation for non-ideal plasma in the Boussinesq approximation for both adiabatic and non-adiabatic perturbations, and in Appendix B we find the analytical solution of this dispersion equation for Keplerian discs at the neutral point.

2 LINEAR ANALYSIS FOR IDEAL FLUID

The dispersion relation for local small axially symmetric disturbances in the simplest case of an ideal fluid without entropy gradients reads (see Balbus & Hawley (1991), Kato, Fukue & Mineshige (1998) and Appendix A for the derivation):

$$\omega_*^4 - \left(\frac{k_z}{k}\right)^2 \kappa^2 \omega_*^2 - 4\Omega^2 \left(\frac{k_z}{k}\right)^2 k_z^2 c_A^2 = 0.$$
 (1)

Here

$$\omega_*^2 = \omega^2 - c_A^2 k_z^2 \,, \tag{2}$$

 $k^2 = k_r^2 + k_z^2,$

$$\kappa^2 = 4\Omega^2 + r\frac{d\Omega^2}{dr} \equiv \frac{1}{r^3}\frac{d\Omega^2 r^4}{dr}$$
(3)

is the epicyclic frequency, and

$$c_A^2 = B_0^2 / (4\pi\rho_0) \tag{4}$$

in the unperturbed Alfvén velocity square. The initial magnetic field B_0 is assumed to be purely poloidal (directed along the *z*-coordinate) and homogeneous.

The solution of the biquadratic equation (1) has the form:

$$\omega^{2} = \left(\frac{k_{z}}{k}\right)^{2} \left[c_{A}^{2}k^{2} + \frac{\kappa^{2}}{2} \pm \sqrt{\frac{\kappa^{4}}{4} + 4\Omega^{2}c_{A}^{2}k^{2}} \right].$$
 (5)

We will examine solutions of this equation by assuming $k_z^2/k^2 \equiv k_z^2/(k_r^2 + k_z^2) = const$, i.e. the direction of the wave vector in the r - z plane is conserved; this is not restrictive for our analysis. Depending on the sign of the root ω^2 , one of three modes can exist: the stable oscillating mode for $\omega^2 > 0$, indifferent equilibrium (neutral) mode for $\omega^2 = 0$, and exponentially growing mode for $\omega^2 < 0$.

According to the classical Rayleigh criterion (Lord Rayleigh 1916), if the epicyclic frequency $\kappa^2 > 0$ (in this case the angular momentum in the flow increases with radius), the equilibrium is stable. If $\kappa^2 < 0$ (the angular momentum decreases with radius), the equilibrium is unstable. If $\kappa^2 = 0$ (the angular momentum does not change with radius), the equilibrium is indifferent.

2.1 Ideal MHD case

Let us start with discussing the behaviour of different modes of dispersion relation (1) in the ideal MHD case. It is instructive to investigate the asymptotics of these modes with decreasing (but nonzero) seed magnetic field (see Section 2.2 for more detail on the limiting transition for vanishing magnetic field).

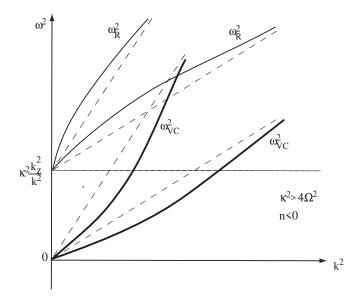


Figure 1. Schematic behaviour of two branches of dispersion equation Eq. (1) ('Reynolds mode' ω_R^2 , thin curves, and 'MRI mode' ω_{VC}^2 , thick curves) for two values of the Alfvén velocity c_A^2 (two values of the seed magnetic field B_0). The dashed straight lines show the asymptotic behaviour of the solutions at large k^2 : $\omega^2 = (k_z/k)^2 c_A^2 k^2$. The smaller the seed magnetic field, the smaller the slope of the asymptotes. Case 1 of the angular velocity and angular momentum increasing with radius ($\kappa^2 > 4\Omega^2$; n < 0).

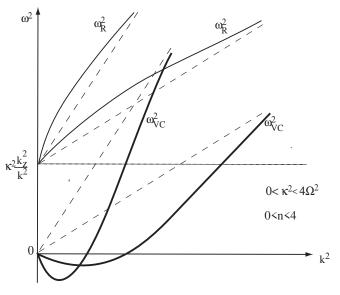


Figure 2. The same as in Fig. 1 for the case of decreasing angular velocity with radius but increasing angular momentum $(0 < \kappa^2 < 4\Omega^2; 0 < n < 4)$ (case 2).

If the magnetic field is present, there are five different types of solutions of Eq. (5) depending on how the angular velocity (angular momentum) changes with radius.

Case 1: $\kappa^2 > 4\Omega^2$, n < 0. In this case there are two stable modes (see Fig. 1), which at large k^2 (short-wavelength limit) tend to the asymptotic behaviour $\omega^2 = (k_z/k)^2 c_A^2 k^2$. With decreasing (but non-zero) seed magnetic field amplitude B_0 (and the corresponding

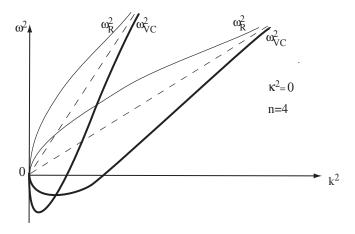


Figure 3. The same as in Fig. 1 for the case of constant angular momentum ($\kappa^2 = 0$; n = 4) (case 3). Both the Rayleigh and MRI branches have infinite derivatives $d\omega^2/dk^2$ at $k^2 = 0$.

unperturbed Alfvén velocity c_A), one mode tends to the classical Rayleigh branch $\omega_R^2 = (k_z/k)^2 \kappa^2$ (the horizontal dashed line in Fig. 1), and the second mode tends to the neutral branch $\omega_{VC}^2 \rightarrow 0$.

Case 2: $0 < \kappa^2 < 4\Omega^2$, 0 < n < 4. In this case the Rayleigh mode ω_R^2 behaves almost in the same way as in case 1 (upper curves in Fig. 2). For the mode ω_{VC}^2 (lower thick curves in Fig. 2) the instability arises in the interval: $0 < k^2 c_A^2 < n\Omega^2$. It is in this case that the MRI instability occurs in a Keplerian accretion disc with n = 3 and $\kappa = \Omega$. With decreasing B_0 the critical wave number separating the stable and unstable behaviour

$$k_{cr}^{2}(\omega^{2}=0) = n \frac{\Omega^{2}}{c_{A}^{2}}$$
(6)

tends to infinity. The maximum instability growth rate characterized by the minimum of the mode ω_{VC}^2 occurs at

$$k_{max}^2 = \frac{n(8-n)}{16} \frac{\Omega^2}{c_A^2} \,. \tag{7}$$

By substituting Eq. (7) into Eq. (5), we find for the MRI mode

$$\omega_{VC,max}^2 = -\frac{n^2}{16} \left(\frac{k_z}{k}\right)^2 \Omega^2 = -\frac{n}{8-n} \left(\frac{k_z}{k}\right)^2 c_A^2 k_{max}^2.$$
 (8)

With decreasing (but non-zero) B_0 and c_A^2 , $\omega_{VC}^2(k_{max}^2) \rightarrow -0$ as $k_{max}^2 \rightarrow \infty$.

Case 3: $\kappa^2 = 0$, n = 4. In this case (see Fig. 3) both the Rayleigh mode ω_R^2 and the MRI mode ω_{VC}^2 go out of zero with infinite derivatives (positive and negative for the Rayleigh and MRI modes, respectively). With finite seed magnetic field, the ω_{VC}^2 mode displays the MRI. As B_0 becomes small (but non-zero), both modes asymptotically approach the neutral mode $\omega^2 \rightarrow 0$.

Case 4: $\kappa^2 < 0$, 4 < n < 8. In this case (see Fig. 4) in the absence of magnetic field the instability according to the Rayleigh criterion takes place (the bottom dashed horizontal line in Fig. 4) with $\omega_R^2 = \kappa^2 (k_z/k)^2$. If the magnetic field is present, the Rayleigh instability is stabilized by the magnetic field at $k^2 > k_{cr}^2$ (bottom thin curves in Fig. 4). Note that k_{cr}^2 and k_{max}^2 here are the same as in Case 2. While similar to the MRI mode, this is now *the Rayleigh mode* ω_R^2 that is unstable and reaches maximum growth rate $\omega_{R,max}^2$ determined by Eq. (8). In contrast, *the Velikhov-Chandrasekhar mode* ω_{VC}^2 (upper thick curves in Fig. 4) remains stable *at all wavenumbers*, and with decreasing (but non-zero) magnetic field $\omega_{VC}^2 \rightarrow +0$.

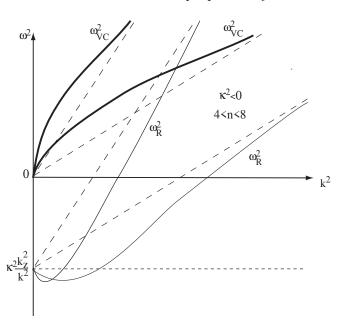


Figure 4. The same as in Fig. 1 for the case of decreasing angular momentum ($\kappa^2 < 0$; 4 < n < 8) (Case 4). Instability according to the Rayleigh criterion occurs. The Rayleigh branch has a negative derivative at $k^2 = 0$.

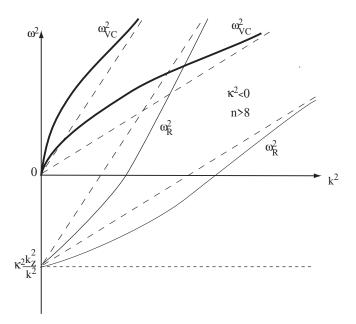


Figure 5. The same as in Fig. 4 for the case ($\kappa^2 < 0$; n > 8) (case 5 in the text); the Rayleigh branch has a positive derivative at $k^2 = 0$.

We stress again that the difference between the Rayleigh and MRI modes is due to their different asymptotic behaviour as $B_0 \rightarrow +0$: the Rayleigh mode is unstable and behaves as $\omega_R \rightarrow -\kappa^2 k_z^2/k^2$, unlike the stable Velikhov-Chandrasekhar mode.

Case 5: $\kappa^2 < 0$, n > 8. The only difference of this case from Case 4 is that the Rayleigh mode ω_R^2 goes out of zero with a positive derivative (bottom thin curves in Fig. 5).

2.2 On the behaviour of MRI at vanishing magnetic field

The transition to purely hydrodynamic case without magnetic field should be treated separately. Let us consider asymptotic solutions (5) for vanishing magnetic field. In the leading order in c_A two branches of the dispersion relation are:

$$\omega_R^2 \simeq \left(\frac{k_z}{k}\right)^2 \left[\kappa^2 + c_A^2 k^2 \left(1 + \frac{4\Omega^2}{\kappa^2}\right)\right],\tag{9}$$

which we have referred to as the Rayleigh mode since in the absence of the magnetic field it tends to the classical Rayleigh mode $\omega_R^2 = (k_z/k)^2 \kappa^2$, and

$$\omega_{VC}^{2} \simeq k_{z}^{2} c_{A}^{2} \left(1 - \frac{4\Omega^{2}}{\kappa^{2}} \right), \qquad (10)$$

which we have referred to as the Velikhov-Chandrasekhar mode and which is manifestly unstable for the Keplerian motion ($\kappa^2 = \Omega^2$).

Notice that unlike the Rayleigh mode, setting magnetic field to zero in Eq. (10) leads to a paradoxical result: $\omega_{VC}^2 = 0$. This 'neutral mode' is fictitious, it does not exist in the purely hydrodynamic case. To see this, let us write linearized system of perfect fluid equations in the Boussinesq approximation (see (A6) – (A9) and Eq. (A13) in Appendix A):

$$k_{r}u_{r} + k_{z}u_{z} = 0$$

$$i\omega u_{r} - 2\Omega u_{\phi} = ik_{r}\frac{p_{1}}{\rho_{0}}$$

$$i\omega u_{\phi} + \frac{\kappa^{2}}{2\Omega}u_{r} = 0$$

$$i\omega u_{z} = ik_{z}\frac{p_{1}}{\rho_{0}}$$
(11)

It is easy to find the dispersion relation in this case:

$$\omega^2 = \left(\frac{k_z}{k}\right)^2 \kappa^2, \qquad (12)$$

which is the classical Rayleigh branch. No neutral mode $\omega^2 = 0$ arises. The neutral mode $\omega = 0$ does exist in the purely hydrodynamic case but only for specific choice of radial perturbations with $u_r = u_z = k_z = 0$ and $-2\Omega u_{\phi} = ik_r(p_1/\rho_0)$ (see (11)). The odd mode $\omega^2 = 0$ arising in the limiting transition with vanishing magnetic field formally appears from Eq. (1) because the fourth order of this dispersion relation is entirely due to the square brackets ~ ω^2 in the denominator of Eq. (A28), which in the case B = 0 cancels with the brackets ~ ω^2 in the nominator.

Similarly, no smooth transition to the hydrodynamic case occurs if viscosity is included (see below). The absence of the smooth transition to the ideal hydrodynamic case when $B \rightarrow 0$ was first noted by Velikhov (1959). At the same time, the transition to the classical Rayleigh mode with vanishing magnetic field occurs smoothly.

3 LINEAR ANALYSIS FOR FLUID WITH VISCOSITY AND MAGNETIC DIFFUSIVITY

Consider the more general case of a non-ideal viscous fluid with finite electric conductivity characterized by the kinematic viscosity coefficient ν and resistivity (magnetic diffusivity) η . Naturally, in problems with viscosity and magnetic diffusivity there is no initial steady state. The angular momentum is redistributed by viscosity on the time scale $\tau_{\nu} \sim R^2/\nu$, and the magnetic field changes on the magnetic diffusion time scale $\tau_{\eta} \sim R^2/\eta$, where *R* is the characteristic size of the system. Everywhere below we will assume these timescales to be extremely long compared to the Keplerian

rotation time and the characteristic instability growth time, if conditions are suitable for the latter to arise. Dispersion relation in this case can be derived following the local linear analysis of MRI performed, e.g., in the monograph Kato, Fukue & Mineshige (1998) with taking into account viscosity and conductivity in the WKBapproximation (see Appendix A, with zero density perturbations Eq. (A13)):

$$\omega_{**}^{4} + \left(\frac{k_{z}}{k}\right)^{2} \left[\left(i\omega + \eta k^{2}\right)^{2} \kappa^{2} + c_{A}^{2} k_{z}^{2} (\kappa^{2} - 4\Omega^{2}) \right] = 0, \qquad (13)$$

where

$$\omega_{**}^2 = -(i\omega + \nu k^2)(i\omega + \eta k^2) - c_A^2 k_z^2.$$
(14)

The dispersion relation (13) is identical to the one derived for a rotating liquid metal annulus in the incompressible limit (Ji, Goodman & Kageyama 2001)¹. This equation was also derived and mathematically analysed in Pessah & Chan (2008). However, that paper focused on the application of the MRI mode to the calculations of the Reynolds and Maxwell stresses in the differentially rotating flow. In what follows we shall discuss the constraints on MRI modes in astrophysical accretion discs, where the free-path length of particles (and hence the viscosity) is limited by the disc thickness.

The magnetic Prandtl number is introduced as $P_m = \nu/\eta$. Using the standard expressions for ν and η for fully ionized hydrogen plasma Spitzer (1962), we readily find

$$P_{\rm m} \approx 3.4 \times 10^{-28} \frac{T^4}{\rho \ln \Lambda_{eH} \Lambda_{pH}}, \qquad (15)$$

where *T* is the temperature, ρ is the density and Λ_{eH} and Λ_{pH} are electron and proton Coulomb logarithms, respectively.

As was shown by Balbus & Henri (2008), the magnetic Prandtl number can be of the order of one in the inner parts of accretion discs around neutron stars and black holes.

3.1 The case of the magnetic Prandtl number $P_m = 1$

Here we will discuss the exact analytic solution to Eq. (13) for the important particular case $P_m = 1$ (which can be derived, for example, from the general analytic solution found in Pessah & Chan (2008)) and obtain restrictions on the maximum mean free-path length of ions in accretion discs at which MRI disappears due to non-ideality effects.

The exact solution of Eq. (13) for $P_m = 1$ is

$$\omega = i\nu k^2 \pm \sqrt{\left(\frac{k_z}{k}\right)^2 \left[c_A^2 k^2 + \frac{\kappa^2}{2} \pm \sqrt{\frac{\kappa^4}{4} + 4\Omega^2 c_A^2 k^2}\right]}.$$
 (16)

Here the plus sign before the second square root corresponds to the Rayleigh branch, and the minus sign corresponds to the Velikhov-Chandrasekhar (MRI) branch. We shall examine below the MRI branch only.

It is noted that the first square root in this equation contains the solutions (5) of Eq. (1):

$$\omega = i \left(\nu k^2 - \sqrt{-\omega_{\nu=0}^2} \right). \tag{17}$$

¹ Note that those authors searched for a stable differential rotation law between cylinders with given viscosity and electric conductivity while we are investigating conditions for MRI in a viscous, electrically conducting flow in gravitational field with given differential rotation law.

On properties of MRI 5

(Here we remind that for regions with MRI $\omega^2 < 0$). Also note that like in the ideal MHD case considered above in Section 2.2, here there are no smooth transition of the MRI mode to the hydrodynamic case with viscosity when vanishing the magnetic field. As can be straightforwardly derived from Eq. (A6)- (A9) in the Appendix, the dispersion relation for the hydrodynamic case with viscosity reads:

$$(i\omega + vk^2)^2 + \left(\frac{k_z}{k}\right)^2 \kappa^2 = 0.$$
 (18)

While the Rayleigh mode (the one with positive sign before the second square root in Eq. (16)) tends to the mode given by Eq. (18) when magnetic field is vanishing, the MRI mode (the one with positive sign before the second square root in Eq. (16)) completely disappears (there is no mode $i\omega + \nu k^2 = 0$ without magnetic field, unless $k_z = 0$).

Below we will consider the case $k_z = k$, i.e. with $k_r = 0$. For further analysis it is convenient to rewrite the dispersion relation (13) in the dimensionless form. We introduce the dimensionless variables:

$$\tilde{\omega} \equiv \omega/\Omega; \quad \tilde{k} \equiv \frac{c_A k}{\Omega}; \quad \tilde{\kappa}^2 \equiv \kappa^2/\Omega^2; \quad \tilde{\nu} \equiv \frac{\nu \Omega}{c_A^2}$$
(19)

For Keplerian discs the dimensionless epicyclic frequency is $\tilde{\kappa}^2 = 1$. In the dimensionless variables, solution to Eq. (13) takes the form:

$$\tilde{\omega} = i \left(\tilde{\nu} \tilde{k}^2 \pm \sqrt{-\tilde{k}^2 - \frac{1}{2} \mp \sqrt{\frac{1}{4} + 4\tilde{k}^2}} \right).$$
(20)

Of the four solutions of Eq. (20) we choose the one for the MRI mode:

$$\tilde{\omega} = i \left(\tilde{\nu} \tilde{k}^2 - \sqrt{-\tilde{k}^2 - \frac{1}{2} + \sqrt{\frac{1}{4} + 4\tilde{k}^2}} \right).$$
(21)

Now we find the neutral point $\tilde{\omega} = 0$. Squaring twice Eq. (21), we obtain the equation for the critical wavenumber \tilde{k}_{cr} separating unstable ($\tilde{k} < \tilde{k}_{cr}$) and stable ($\tilde{k} > \tilde{k}_{cr}$) perturbations:

$$\tilde{\nu}^4 \tilde{k}^6 + 2\tilde{\nu}^2 \tilde{k}^4 + (1 + \tilde{\nu}^2)\tilde{k}^2 - 3 = 0.$$
(22)

Without viscosity we recover the old result: $\tilde{k}_{cr}^2 = 3$ (see Eq. (6)). It is easy to check that for the dimensionless viscosity $\tilde{\nu} = 4/5$ the neutral point is $\tilde{k}_{cr} = \sqrt{15/16}$, i.e. here the neutral point coincides with the maximum wavenumber k_{max} at which the maximum MRI growth occurs in the inviscid case (see Eq. (7) above). At large dimensionless viscosity $\tilde{\nu} \gg 1$, the asymptotic solution of Eq. (21) reads

$$\tilde{k}_{cr} \simeq \frac{\sqrt{3}}{\tilde{\nu}} \,. \tag{23}$$

Therefore, at arbitrarily high viscosity there exists the interval of wavenumbers $0 < \tilde{k} < \tilde{k}_{cr}$ where MRI is still takes place, but the MRI increment here is very small.

Actually, in realistic accretion discs with finite thickness *H* we should take into account that there is the lower limit for *k* corresponding to the obvious restriction on the maximum perturbation wavelength $\lambda < 2H$:

$$k = \frac{2\pi}{\lambda} > \frac{\pi}{H} \equiv k_{min} \,. \tag{24}$$



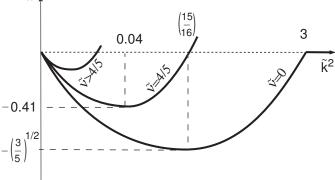


Figure 6. Schematics of the influence of viscosity on the MRI condition $0 < \tilde{k} < \tilde{k}_{cr}$. Shown are curves of the imaginary part of $\tilde{\omega}$ as a function of the dimensionless wave number \tilde{k}^2 . With increasing viscosity, the MRI interval shifts to the left and shrink (see also Fig. 1 in Pessah & Chen (2008)).

Therefore, in the dimensionless variables we find the MRI condition in the form:

$$\tilde{k}_{min} \leqslant \tilde{k} \leqslant \tilde{k}_{cr} \,. \tag{25}$$

It is also convenient to change from the disc thickness H to the characteristic thermal velocity in the disc $c_{s,s}$ since in accretion discs the hydrostatic equilibrium along the vertical coordinate yields

$$c_s = \Pi \Omega H \tag{26}$$

where Π is a numerical coefficient. For example, in the standard geometrically thin Shakura-Sunyaev α -disk $\Pi = 1/\sqrt{4\Pi_1} \simeq 1/\sqrt{20}$ (see Ketsaris & Shakura (1998)). Then in the inviscid fluid $\tilde{k}_{cr} = \sqrt{3}$, $\tilde{k}_{min} = \pi \Pi(c_A/c_s)$, and the MRI condition Eq. (25) takes the form

$$\pi \Pi \left(\frac{c_A}{c_s}\right) \leqslant \sqrt{3} \,. \tag{27}$$

Essentially, this is the well-known condition that for MRI to operate the seed magnetic field should not exceed some critical value.

In the non-ideal plasma the MRI condition Eq. (27) becomes

$$\pi \Pi \left(\frac{c_A}{c_s}\right) \leqslant \tilde{k}_{cr} \,. \tag{28}$$

Note that \tilde{k}_{cr} decreases with \tilde{v} . For example, if \tilde{v} is high, Eq. (23) implies very small values of \tilde{k}_{cr} and, correspondingly, very low c_A at which MRI can occur with uninterestingly small increments. The schematic behaviour of the MRI mode at non-zero viscosity is shown in Fig. 6. At arbitrary finite viscosity \tilde{v} the neutral point $\tilde{\omega}(\tilde{k}_{cr})$ separates exponentially growing small perturbations $\propto exp(i\omega t)$ (the lower part of Fig. 6 where Im $\tilde{\omega} > 0$) from exponentially decaying ones (the upper part of Fig. 6). At zero viscosity, however, the function $\tilde{\omega}(\tilde{k})$ (the curve labeled by $\tilde{v} = 0$) ends at the point $\tilde{k}_{cr} = \sqrt{3}$, because in this case at $\tilde{k} \ge k_{cr}$ the $\tilde{\omega}$ becomes purely real and small perturbations oscillate.

In the case of high viscosity it is convenient to express the ratio c_A/c_s through the dimensionless viscosity \tilde{v} . Using the conventional definition of the viscosity coefficient $v = c_s l$, where l is the effective mean-free path of ions with account for the Coulomb logarithm, and our convention for the thermal velocity in the disc

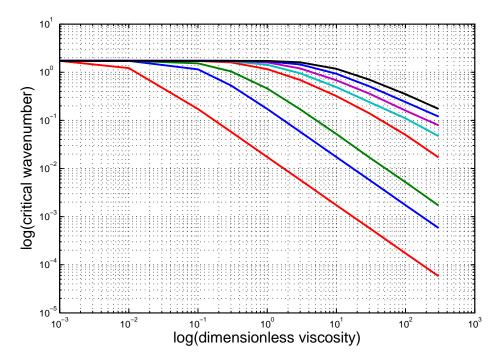


Figure 7. Dimensionless critical wavenumber \tilde{k}_{cr} as a function of dimensionless viscosity coefficient $\tilde{\nu}$ for different magnetic Prandtl numbers P_m. Lines from bottom to top correspond to P_m=0.01, 0.1, 0.3, 3, 10, 300, 100, 300.

(26) introduced above, we find:

$$\tilde{\nu} \equiv \nu \frac{\Omega}{c_A^2} = \frac{1}{\Pi} \left(\frac{c_s}{c_A} \right)^2 \left(\frac{l}{H} \right).$$
(29)

Finally, we obtain the MRI condition in the convenient form:

$$\frac{l}{H} \leq \frac{1}{\pi^2 \Pi} \tilde{\nu} \tilde{k}_{cr}^2 \,. \tag{30}$$

In the particular case $P_m=1$ we can explicitly find $\tilde{\nu}\tilde{k}_{cr}^2$ from Eq. (21):

$$\tilde{\nu}\tilde{k}_{cr}^2 = \sqrt{-\tilde{k}_{cr}^2 - \frac{1}{2} + \sqrt{\frac{1}{4} + 4\tilde{k}_{cr}^2}},$$
(31)

so that condition (30) takes the form:

$$\frac{l}{H} \leq \frac{1}{\pi^2 \Pi} \sqrt{-\tilde{k}_{cr}^2 - \frac{1}{2} + \sqrt{\frac{1}{4} + 4\tilde{k}_{cr}^2}}.$$
(32)

(This formula should be used when $\nu \neq 0$, i.e. when $\tilde{k}_{cr}^2 < 3$). Consider first the case of small viscosities where $\tilde{k}_{cr}^2 \approx 3$. By introducing the small parameter $\epsilon = 3 - \tilde{k}_{cr}^2 \ll 1$ and expanding the left-hand side of Eq. (32) in ϵ , we obtain

$$\frac{l}{H} \le \frac{1}{\pi^2 \Pi} \sqrt{\frac{41}{49}\epsilon} \,. \tag{33}$$

Now consider the special case where \tilde{k}_{cr} coincides with the wavenumber of maximum MRI increment in the ideal fluid: $\tilde{k}_{cr} = \tilde{k}_{max} = \sqrt{\frac{15}{16}}$ (see Eq. (7)). This is realized at $\tilde{\nu} = 4/5$. Here we find the limit

$$\left(\frac{l}{H}\right) \leq \frac{1}{\pi^2 \Pi} 0.75 \approx 0.34. \tag{34}$$

Finally, in the high-viscosity limit for $P_m=1 \tilde{\nu} \gg 1$, substituting the asymptotic (23) into Eq. (30) with account for the expression for dimensionless viscosity (29) we obtain

$$\left(\frac{l}{H}\right) \leq \frac{\sqrt{3}}{\pi} \left(\frac{c_A}{c_s}\right), \quad \mathbf{P}_{\mathrm{m}} = 1, \tilde{\nu} \gg 1.$$
 (35)

Note that this constraint is insensitive to the disc vertical structure parameter Π . This condition can be checked for particular microphysics plasma properties in different thin Keplerian discs.

3.2 The case of arbitrary magnetic Prandtl number

The generalization of the above analysis to an arbitrary Prandtl number is straightforward. First, for given P_m and $\tilde{\nu}$ we solve the dimensionless Eq. (13) to find $\tilde{k}_{cr}(\tilde{\nu}, P_m)$ (see Appendix B), and then obtain the general MRI condition (28)

$$\left(\frac{c_A}{c_s}\right) \leqslant \frac{1}{\pi \Pi} \tilde{k}_{cr}(\tilde{\nu}, \mathbf{P}_{\mathrm{m}}) \,. \tag{36}$$

The result of calculation of \tilde{k}_{cr} for a range of magnetic Prandtl numbers P_m and dimensionless viscosities $\tilde{\nu}$ can be found in Pessah & Chan (2008) (see e.g. their Fig. 6 and 7) and is illustrated in Fig. 7.

In the limiting case of high dimensionless viscosities $P_m/\tilde{\nu}^2 \ll$ 1, which can be realized in the outer parts of thin Keplerian accretion discs (see Eq. (15) above), using asymptotic (B6) and definition (29), we find the restriction on the mean-free path of ions in the disc

$$\left(\frac{l}{H}\right) \leq \frac{\sqrt{3} \mathbf{P}_{\mathrm{m}}}{\pi} \left(\frac{c_{A}}{c_{s}}\right), \quad \mathbf{P}_{\mathrm{m}}/\tilde{\nu}^{2} \ll 1.$$
(37)

which is the generalization of Eq. (35) for arbitrary magnetic

Prandtl number. Using the expression for the dimensionless viscosity (29), the condition for the power-law asymptotic $P_m/\tilde{\nu}^2 \ll 1$ can be recast to the inequality

$$P_{\rm m}/\tilde{\nu}^2 \ll 1 \iff \left(\frac{l}{H}\right)^2 \gg \Pi P_{\rm m} \left(\frac{c_A}{c_s}\right)^4$$
. (38)

Therefore, the MRI condition can be written in terms of the interval for l/H in a Keplerian disc as

$$\sqrt{\Pi P_{\rm m}} \left(\frac{c_A}{c_s}\right)^2 \ll \left(\frac{l}{H}\right) \leqslant \frac{\sqrt{3} P_{\rm m}}{\pi} \left(\frac{c_A}{c_s}\right).$$
 (39)

4 DISCUSSION AND CONCLUSION

In the present paper we have extended the original analysis of MRI in ideal MHD plasmas carried out by Balbus (2012). First, we emphasize that hydromagnetic flows in which the angular momentum increases or decreases with radius are different from the point of view of the MRI development. In the classical Rayleighunstable case where the angular momentum decreases with radius, the Velikhov-Chandrasekhar MRI mode is stable, while the Rayleigh mode is unstable (see Fig 4, 5); the magnetic field stabilizes the Rayleigh mode in the short-wavelength limit. When the angular momentum in the flow increases with radius, MRI arises at long wavelengths (small wave numbers k, see Fig. 2). However, the local WKB approximation should be applied with caution at long wavelengths. At long wavelengths, the ansatz for the solution should be rather taken in the global form $f(r)e^{i(\omega t - k_r r - k_z z)}$. Note that the original papers by Velikhov and Chandrasekhar analyzed the linear stability of magnetized flows between cylinders exactly in that approximation (see also Sano & Miyama (1999) for the global analysis of perturbations in an inviscid magnetized proto-planetary discs with non-zero magnetic diffusivity).

Second, in the phenomenologically interesting case of thin Keplerian accretion discs, viscosity may restrict MRI growth. This situation can be realized in the inner parts of accretion discs. Indeed, at high temperatures the mean free path of ions $l \sim T^2$ can become comparable with the characteristic disc thickness H at H < r (thin discs). This means that the flow should be treated kinetically (see, for example, recent 2.5D hybrid calculations Shirakawa & Hoshino (2014) or the discussion of MRI in rarefied astrophysical plasmas with Braginskii viscosity in Islam & Balbus (2005)). The seed small magnetic field under these conditions does not grow, i.e. the high ion viscosity can suppress MRI. Clearly, this interesting regime requires further study.

At large magnetic Prandtl numbers $P_m \gg 1$, which can be realized in the innermost parts of accretion discs around neutron stars and black holes, the kinematic viscosity v is much larger than the magnetic diffusivity η . In this case plasma may become collisionless, and hydrodynamic description fails. Our analysis shows that in principle the collisionless regime (the ion mean-free path comparable to or larger than the disc thickness, $l \sim H$) in Keplerian discs can be realized even for magnetic Prandtl numbers $P_m \simeq 1$ (see Eq. (39)).

We have also obtained the dispersion relation for local small perturbations in the Boussinesq limit for non-adiabatic perturbations (see Eq. (A32)). This is the fifth-order algebraic equation, in contrast to the fourth-order dispersion relation for adiabatic perturbations or non-adiabatic perturbations with $k_r = 0$ in non-ideal plasma (13). Also note that when the density perturbations are expressed through the entropy gradients (see Eq. (2.2h) in

On properties of MRI 7

Balbus & Hawley (1991)), the frequency appears in the denominator but the final dispersion relation (2.5) in Balbus & Hawley (1991) remains to be the fourth-order equation in ω even with taking into account the entropy gradients. Apparently, the difference is due to the fact that in the case of non-adiabatic perturbations the density variations are proportional to the azimuthal velocity perturbations u_{ϕ} (see our Eq. (A21)) and not to u_z and u_r as in the case considered by Balbus & Hawley (1991). The analysis of the effect of non-adiabatic perturbations deserves a separate study and will be addressed in a future work.

Perturbations with $k_r = 0$ represent waves propagating along the *z*-coordinates, and when their wavelength is comparable to the disc thickness, the WKB approximation becomes problematic. Perturbations with $k_z = 0$ propagate along the *r*-coordinate, which is much larger than the disc thickness for thin accretion discs. However, for such perturbations with $k = k_r$ and $k_z = 0$ the second term in Eq. (13) and Eq. (A32) vanishes, and therefore from Eq. (14) we find two perturbation modes

$$\omega_1 = i\nu k^2, \quad \omega_2 = i\eta k^2, \tag{40}$$

i.e. decaying standing waves for any seed magnetic field. This may suggest that in the poloidal magnetic fields purely radial perturbations with $k = k_r$ do not grow. The situation is different when the azimuthal magnetic field is present. This case should be considered separately and has been investigated for a range of astrophysical applications in other papers (see, e.g., Acheson (1978); Sano & Miyama (1999); Ruediger et al. (2014); Kirillov, Stefani & Fukumoto (2014)).

We conclude that in thin Keplerian accretion discs the adding of viscosity can strongly restrict the MRI conditions once the mean free path of ions becomes comparable with the disc thickness. These limitation should be taken into account in the direct numerical simulations of MRI in astrophysical accretion discs.

5 ACKNOWLEDGEMENTS

We thank the anonymous referee for drawing our attention to earlier papers by Pessah & Chan (2008), Islam & Balbus (2005) and Masada & Sano (2008) and for the constructive criticism. We also thank Prof. Dr. F. Meyer for discussions and MPA (Garching) for hospitality. The work was supported by the Russian Science Foundation grant 14-12-00146.

APPENDIX A: DERIVATION OF THE DISPERSION EQUATION FOR NON-IDEAL PLASMA

Here we generalize the derivation of the MRI dispersion equation (1) given in Kato, Fukue & Mineshige (1998) for the case of nonideal plasma with arbitrary kinetic coefficients v and η (see also Ji, Goodman & Kageyama (2001)).

The system of non-deal MHD equations reads:

1) mass conservation equation

$$\frac{\partial \rho}{\partial t} + \nabla \cdot (\rho \boldsymbol{u}) = 0, \qquad (A1)$$

2) Navier-Stokes equation including gravity force and Lorentz force

$$\frac{\partial \boldsymbol{u}}{\partial t} + (\boldsymbol{u}\nabla) \cdot \boldsymbol{u} = -\frac{1}{\rho}\nabla p - \nabla \phi_g + \frac{1}{4\pi\rho}(\nabla \times \boldsymbol{B}) \times \boldsymbol{B} + \nu \Delta \boldsymbol{u} \quad (A2)$$

(here ϕ_g is the Newtonian gravitational potential),

3) induction equation

$$\frac{\partial \boldsymbol{B}}{\partial t} = \nabla \times (\boldsymbol{u} \times \boldsymbol{B}) + \eta \Delta \boldsymbol{B}, \qquad (A3)$$

4) energy equation

$$\frac{\rho \mathcal{R}T}{\mu} \left[\frac{\partial s}{\partial t} + (\boldsymbol{u} \nabla) \cdot \boldsymbol{s} \right] = Q_{visc} - \nabla \cdot \boldsymbol{F} + \frac{\eta}{4\pi} [\nabla \times \boldsymbol{B}]^2 \,. \tag{A4}$$

where *s* is the specific entropy (per particle), \mathcal{R} is the universal gas constant, μ is the molecular weight, *T* is the temperature, and terms on the right stand for viscous, energy flux *F* and Joule dissipation, respectively.

5) These equations should be completed with the equation of state for a perfect gas, which is convenient to write in the form:

$$p = K e^{s/c_V} \rho^{\gamma} , \qquad (A5)$$

where *K* is a constant, c_V is the specific volume heat capacity and $\gamma = c_p/c_V$ is the adiabatic index (5/3 for the monoatomic gas).

We will consider small axially symmetric perturbations in the WKB approximation with space-time dependence $e^{i(\omega t - k_r r - k_z z)}$, where r, z, ϕ are cylindrical coordinates. The unperturbed magnetic field is assumed to be purely poloidal: $B_0 = (0, 0, B_0)$. The velocity and magnetic field perturbations are $\boldsymbol{u} = (u_r, u_{\phi}, u_z)$ and $\boldsymbol{b} = (b_r, b_{\phi}, b_z)$, respectively. The density, pressure and entropy perturbations are ρ_1 , p_1 , and s_1 over the unperturbed values ρ_0 , p_0 , and s_0 , respectively. To filter out magnetoacoustic oscillations arising from the restoring pressure force, we will use the Boussinesq approximation, i.e. consider incompressible gas motion $\nabla \cdot \boldsymbol{u} = 0$. In the energy equation we neglect Eulerian pressure variations, $p_1(t, r, \phi, z) = 0$, but Lagrangian pressure variations $\delta p(t, r(t_0), \phi(t_0, z(t_0)))$ are non-zero. (We remind that for infinitesimally small shifts the perturbed gas parcel acquires the pressure equal to that of the ambient medium; see e.g. Spiegel & Veronis (1960); Kundu, Cohen & Dowling (2012) for discussion of the Boussinesq approximation).

In the linear approximation, the system of differential nonideal MHD equations is reduced to the following system of algebraic equations.

a) The Boussinesq approximation for gas velocity \boldsymbol{u} is $\nabla \cdot \boldsymbol{u} = 0$:

$$k_r u_r + k_z u_z = 0. (A6)$$

b) The radial, azimuthal and vertical components of the Euler momentum equation are, respectively:

$$i\omega u_r - 2\Omega u_{\phi} = ik_r \frac{p_1}{\rho_0} - \frac{\rho_1}{\rho_0^2} \frac{\partial p_0}{\partial r} + i\frac{c_A^2}{B_0}(k_r b_z - k_z b_r) - vk^2 u_r ,$$
 (A7)

$$i\omega u_{\phi} + \frac{\kappa^2}{2\Omega} u_r = -i \frac{c_A^2}{B_0} k_z b_{\phi} - \nu k^2 u_{\phi} , \qquad (A8)$$

$$i\omega u_z = ik_z \frac{p_1}{\rho_0} - \frac{\rho_1}{\rho_0^2} \frac{\partial p_0}{\partial z} - \nu k^2 u_z \tag{A9}$$

Here $k^2 = k_r^2 + k_z^2$ so that in the linear order $v\Delta u \rightarrow -vk^2 \{u_r, u_\phi, u_z\}^2$, and we have introduced the unperturbed Alfvén velocity $c_A^2 = B_0^2/(4\pi\rho_0)$.

² Here we neglect terms ~ (k_r/r) compared to terms ~ k^2 , see also discussion in Acheson (1978).

To specify density perturbations ρ_1/ρ_0 , we need to address the energy equation. First, consider adiabatic perturbations, i.e. require

$$\frac{\partial s}{\partial t} + (\boldsymbol{u} \cdot \nabla) s = 0.$$
 (A10)

For small density perturbations from Eq. (A5) we obtain for entropy perturbations

$$\frac{s_1}{c_V} + \gamma \frac{\rho_1}{\rho_0} = 0,$$
 (A11)

and after substituting this into Eq. (A10) we get

$$i\omega\gamma\frac{\rho_1}{\rho_0} + u_z\frac{\partial\ln p\rho^{-\gamma}}{\partial z} + u_r\frac{\partial\ln p\rho^{-\gamma}}{\partial r} = 0$$
(A12)

(cf. Eq. (122) in Balbus & Hawley (1998)). Hence in the absence of entropy gradients we obtain

$$\frac{1}{\rho_0}\frac{\partial\rho_1}{\partial t} = 0.$$
 (A13)

Consider now the more general case of *non-adiabatic* linear perturbations. To do this, we need to specify the right-hand side of the energy equation (A4). Let us start with the last term. Writing for the magnetic field $\mathbf{B} = \mathbf{B}_0 + \mathbf{b}$ and taking into account that for the unperturbed field $\nabla \times \mathbf{B}_0 = 0$, we see that the Joule dissipation term is quadratic in magnetic field perturbations \mathbf{b} , so we exclude it from consideration. The heat flux divergence is

$$\nabla \cdot \boldsymbol{F} = \nabla(-\kappa_T \nabla T) = -\kappa_T \Delta T , \qquad (A14)$$

where κ_T is the temperature conductivity coefficient. From equation of state for ideal gas written in the form $p = \rho R T / \mu$, we find for small perturbations with zero Eulerian pressure variations $p_1/p_0 =$ 0

$$\frac{\rho_1}{\rho_0} = -\frac{T_1}{T_0},$$
 (A15)

i.e. in the axially symmetric waves considered here the density variations are in counter-phase with temperature variations.

The viscous dissipative function Q_{visc} can be written as $Q_{visc} = \rho v \Phi$, where the function Φ in polar coordinates is

$$\Phi = 2\left[\left(\frac{\partial u_r}{\partial r}\right)^2 + \left(\frac{1}{r}\left(\frac{\partial u_{\phi}}{\partial \phi}\right) + \frac{u_r}{r}\right)^2 + \left(\frac{\partial u_z}{\partial z}\right)^2\right] \\ + \left[r\frac{\partial}{\partial r}\left(\frac{u_{\phi}}{r}\right) + \frac{1}{r}\frac{\partial u_r}{\partial \phi}\right]^2 + \left[\frac{1}{r}\frac{\partial u_z}{\partial \phi}\right]^2 \\ + \left[\frac{\partial u_r}{\partial z} + \frac{\partial u_z}{\partial r}\right]^2 - \frac{2}{3}(\nabla \cdot \boldsymbol{u})^2.$$
(A16)

All terms but one in this function are quadratic in small velocity perturbations; this term has the form:

$$\nu \rho \left(\frac{\partial u_{\phi}}{\partial r} - \frac{u_{\phi}}{r}\right)^2. \tag{A17}$$

Writing for the azimuthal velocity $u_{\phi} = u_{\phi,0} + u_{\phi,1}$ (here for the purposes of this paragraph and only here we specially mark the unperturbed velocity with index 0, not to be confused with our notations u_{ϕ} for perturbed velocity in Eq. (A7)-Eq. (A8) above and below). Thus we obtain for the viscous dissipation

$$Q_{visc} = v\rho r \frac{d\Omega}{dr} \left[r \frac{d\Omega}{dr} - 2ik_r u_{\phi,1} - 2\frac{u_{\phi,1}}{r} \right] + \text{quadratic terms}.$$
(A18)

Here $\Omega = u_{\phi,0}/r$ is the angular (Keplerian) velocity of the unperturbed flow. The first term in parentheses describes the viscous energy release in the unperturbed Keplerian flow. For this unperturbed flow we have

$$\frac{\partial s_0}{\partial t} = \nu \mu \frac{[r(d\Omega/dr)]^2}{\mathcal{R}T} = \frac{9}{4} \nu \mu \frac{\Omega^2}{\mathcal{R}T} \,. \tag{A19}$$

Thus, the entropy of the unperturbed flow changes along the radius. However, on the scale of the order of or smaller than the disc thickness, the entropy gradient can be neglected. The second term in Eq. (A18) vanishes if $k_r = 0$, i.e. we consider two-dimensional perturbations with only $k_z \neq 0$. As a result, the energy equation with zero entropy gradients in the Boussinesq limit becomes

$$\frac{\rho_0 \mathcal{R} T_0}{\mu} s_1 = -2ik_r v \rho_0 r \frac{d\Omega}{dr} u_{\phi,1} - \kappa_T k^2 T_0 \frac{T_1}{T_0} \,. \tag{A20}$$

Like in the linearized equation $\nabla \cdot \boldsymbol{u} = 0$, here we have neglected the term $u_{\phi,1}/r$. By substituting Eq. (A11) and Eq. (A15) into Eq. (A20), we find the relation between the density variations and u_{ϕ} in the in the Boussinesq limit with zero entropy gradients:

$$\frac{\rho_1}{\rho_0} \left(i\omega c_p + \frac{\kappa_T k^2}{\rho_0 \mathcal{R}/\mu} \right) = \frac{2ik_r v r(d\Omega/dr)}{\mathcal{R}T_0/\mu} u_\phi \tag{A21}$$

Here $c_p = \gamma c_V = \gamma/(\gamma - 1)$ is the specific heat capacity (per particle) at constant pressure.

To describe the effects of thermal conductivity, it is convenient to introduce the usual dimensionless Prandtl number:

$$\Pr \equiv \frac{\nu \rho_0 C_p}{\kappa_T} \,. \tag{A22}$$

(Here $C_p = c_p \mathcal{R}/\mu$). Substituting Eq. (A22) into Eq. (A21) yields:

$$\frac{\rho_1}{\rho_0} = \frac{\gamma/(\gamma - 1)}{(i\omega + \nu k^2/\text{Pr})} \frac{2ik_r \nu r(d\Omega/dr)}{\Re T_0/\mu} u_\phi \tag{A23}$$

It is straightforward to include the density perturbations in the non-adiabatic case (A21) in the analysis. This significantly complicates the final dispersion equation (see Eq. (A32) below). We stress again that the two-dimensional case with $k_r = 0$ produces the dispersion relation for small local perturbations which is *exact* even in the case of non-adiabatic perturbations.

c) The three components of the induction equation with account for $\eta \Delta B \rightarrow -\eta k^2 \{b_r, b_\phi, b_z\}$ read:

$$i\omega b_r = -iB_0k_z u_r - \eta k^2 b_r, \qquad (A24)$$

$$i\omega b_{\phi} = -iB_0 k_z u_{\phi} + r \frac{d\Omega}{dr} b_r - \eta k^2 b_{\phi} , \qquad (A25)$$

$$i\omega b_z = iB_0 k_r u_r - \eta k^2 b_z \,. \tag{A26}$$

Following Kato, Fukue & Mineshige (1998), we express all perturbed quantities through u_{c} :

$$u_r = -\frac{k_z}{k_r} u_z \,, \tag{A27}$$

$$u_{\phi} = \frac{k_z}{k_r} \frac{\frac{\kappa^2}{2\Omega} (i\omega + \eta k^2)^2 + c_A^2 k_z^2 r \frac{d\Omega}{dr}}{\left[(i\omega + \nu k^2) (i\omega + \eta k^2) + c_A^2 k_z^2 \right] (i\omega + \eta k^2)} u_z \,, \tag{A28}$$

$$\frac{b_r}{B_0}(i\omega + \eta k^2) = i\frac{k_z^2}{k_r}u_z, \qquad (A29)$$

$$\frac{b_{\phi}}{B_0}(i\omega + \eta k^2) = -ik_z u_{\phi} + \frac{ir\frac{d\Omega}{dr}}{(i\omega + \eta k^2)}\frac{k_z^2}{k_r}u_z, \qquad (A30)$$

$$\frac{b_z}{B_0}(i\omega + \eta k^2) = -ik_z u_z, \qquad (A31)$$

On properties of MRI 9

The system of linear equations (A6) and (A27)- (A31) contains the equation $\nabla \cdot \boldsymbol{b} = 0$. Indeed, by multiplying Eq. (A29) and Eq. (A31) by k_r and k_z , respectively, and summing up the obtained equations, we get $k_r b_r + k_z b_z = 0$. Substituting Eq. (A27)-Eq. (A31) into Eq. (A7) and rearranging the terms, we arrive at the dispersion relation (13).

The dispersion relation in the general case of non-adiabatic perturbations with $k_r \neq 0$, i.e. with non-vanishing density perturbations ρ_1 (see Eq. (A21)) is:

$$\omega_{**}^{4} + \left(\frac{k_z}{k}\right)^2 \quad \left[\left(i\omega + \eta k^2\right)^2 \kappa^2 + c_A^2 k_z^2 (\kappa^2 - 4\Omega^2)\right] \\ \left[1 - \frac{\gamma - 1}{\gamma} \frac{ik_r}{(i\omega + \gamma k^2/\Pr)} \left(A - \frac{k_r}{k_z}B\right)\right] = 0, \quad (A32)$$

where ω_{**} is determined by Eq. (14) in the main text and

$$A = \nu \left(\frac{d\ln\Omega}{d\ln r}\right) \left(\frac{1}{p_0} \frac{dp_0}{dr}\right); \quad B = \nu \left(\frac{d\ln\Omega}{d\ln r}\right) \left(\frac{1}{p_0} \frac{dp_0}{dz}\right).$$
(A33)

Although the terms with *A* and *B* arising from the viscous dissipation function are proportional to $(k_r/r)(\nu/\omega)$ and $(k_r^2/k_z r)(\nu/\omega)$, they are retained in our analysis because at large viscosity they can be comparable to or even higher than one. The expression in the square brackets in Eq. (A32) above can be rewritten in the equivalent form:

$$\left[1 + \frac{\gamma - 1}{\gamma} \frac{i\nu}{(i\omega + \nu k^2/\Pr)} \left(\frac{k_r}{k_z}\right) \frac{d\ln\Omega/d\ln r}{\mathcal{R}T_0/\mu} (k_z g_{r,eff} - k_r g_z)\right],$$
(A34)

where $g_{r,eff} = -1/\rho_0(dp_0/dr)$ and $g_z = -1/\rho_0(dp_0/dz)$ are the effective radial and vertical gravity accelerations in the unperturbed flow, respectively. Clearly, for $k_r = 0$ we return to Eq. (13) with $k = k_z$. Note that for $k_r \neq 0$ Eq. (A32) is a fifth-order algebraic equation. For perturbations with $k_r = 0$ this equation becomes a fourth-order algebraic equation, which already has exponentially growing MRI modes. For completeness, it would be desirable to investigate this five-order equation. However, in the absence of the magnetic field Eq. (A32) turns into a third-order algebraic equation. As we show in the subsequent paper (Shakura & Postnov 2014, submitted), one of the Rayleigh modes in this case becomes exponentially unstable at long wavelengths even in the Rayleigh-stable case of Keplerian rotation.

APPENDIX B: ANALYTICAL SOLUTION FOR THE CRITICAL WAVE NUMBER \tilde{K}_{CR} IN THE GENERAL CASE OF NON-IDEAL PLASMA

Here we provide the analytical solution of Eq. (13) for arbitrary magnetic Prandtl number P_m and dimensionless viscosity coefficient \tilde{v} at the neutral point where $\tilde{\omega}(\tilde{k}_{cr}) = 0$. To do this, it is convenient, for the sake of brevity, to introduce new dimensionless variables

$$y \equiv \tilde{k}^2, \quad X = i\tilde{\omega} + \tilde{\nu}y$$
 (B1)

and rewrite dimensionless dispersion relation (13) in the equivalent form:

$$X^{4} + 2\frac{1-P_{m}}{P_{m}}\tilde{v}yX^{3} + \left[\left(\frac{1-P_{m}}{P_{m}}\right)^{2}\tilde{v}^{2}y^{2} + 2y + 1\right]X^{2} + \left[\frac{1-P_{m}}{P_{m}}\tilde{v}y(y+1)\right]X + \left(\frac{1-P_{m}}{P_{m}}\right)^{2}\tilde{v}^{2}y^{2} + y^{2} - 3y = 0.$$
 (B2)

(Here we assumed Keplerian discs with $\tilde{\kappa} = 1$ and used $k_z/k = 1$). Noticing that at the neutral point determined by the condition

 $\tilde{\omega}(y_{cr}) = 0$ we have $X = \tilde{\nu}y_{cr}$, we arrive at the equation for y_{cr} :

$$y_{cr} \left[\tilde{\nu}^4 y_{cr}^3 + \tilde{\nu}^2 y_{cr} (2y_{cr} \mathbf{P}_{\rm m} + 1) + \mathbf{P}_{\rm m}^2 (y_{cr} - 3) \right] = 0.$$
 (B3)

At $P_m = 1$ this equation, of course, coincides with Eq. (22). The non-trivial real solution to the cubic equation in the square brackets of Eq. (B3) reads:

$$y_{cr} \equiv \tilde{k}_{cr}^2 = \mathcal{A} - \frac{2P_{\rm m}}{3\tilde{v}^2} - \frac{1}{\mathcal{A}} \left(\frac{1}{3\tilde{v}^2} - \frac{P_{\rm m}^{-2}}{9\tilde{v}^4} \right),$$
 (B4)

where

$$\mathcal{A} = \left[\left(\frac{1}{27\bar{v}^6} + \frac{2P_m^2}{27\bar{v}^8} + \frac{P_m^3}{\bar{v}^8} + \frac{9P_m^4}{4\bar{v}^8} + \frac{P_m^4}{27\bar{v}^{10}} + \frac{P_m^5}{9\bar{v}^{10}} \right)^{1/2} + \frac{P_m}{3\bar{v}^4} + \frac{3P_m^2}{2\bar{v}^4} + \frac{P_m^3}{27\bar{v}^6} \right]^{1/3} .$$
(B5)

At high dimensionless viscosities there is an asymptotic to the solution (B4) for $P_m/\tilde{\nu}^2 \ll 1$:

$$y_{cr} = \tilde{k}_{cr}^2 \approx \frac{3P_{\rm m}^2/\tilde{\nu}^2}{1 + P_{\rm m}^2/\tilde{\nu}^2} = \frac{3P_{\rm m}^2}{\tilde{\nu}^2} + O\left(\frac{P_{\rm m}^2}{\tilde{\nu}^2}\right)^2.$$
 (B6)

Note that this asymptotic can be also found in Pessah & Chan (2008) (their Eq. (97)) and for small P_m can be derived for Keplerian rotation and $k = k_z$ from Eq. (3) in Ji, Goodman & Kageyama (2001).

REFERENCES

- Acheson D. J., 1978, Royal Society of London Philosophical Transactions Series A, 289, 459
- Balbus S. A., 2004, ApJ, 616, 857
- Balbus S. A., 2012, MNRAS, 423, L50
- Balbus S. A., Hawley J. F., 1991, ApJ, 376, 214
- Balbus S. A., Hawley J. F., 1998, Reviews of Modern Physics, 70, 1
- Balbus S. A., Henri P., 2008, ApJ, 674, 408
- Chandrasekhar S., 1960, Proceedings of the National Academy of Science, 46, 253
- Hawley J. F., Gammie C. F., Balbus S. A., 1995, ApJ, 440, 742
- Hawley J. F., Richers S. A., Guan X., Krolik J. H., 2013, ApJ, 772, 102
- Islam T., Balbus S., 2005, ApJ, 633, 328
- Ji H., Goodman J., Kageyama A., 2001, MNRAS, 325, L1
- Kato S., Fukue J., Mineshige S., eds., 1998, Black-hole accretion disks
- Ketsaris N. A., Shakura N. I., 1998, Astronomical and Astrophysical Transactions, 15, 193
- Kirillov O. N., Stefani F., Fukumoto Y., 2014, Journal of Fluid Mechanics, 760, 591
- Kotko I., Lasota J.-P., 2012, A&A, 545, A115
- Kundu P. K., Cohen I. M., Dowling D. R., 2012, Fluid Mechanics, 5th edn. Academic Press, Boston
- Lord Rayleigh, 1916, Proc. R. Soc. A, 93, 143
- Masada Y., Sano T., 2008, ApJ, 689, 1234
- Nauman F., Blackman E. G., 2015, MNRAS, 446, 2102
- Pessah M. E., Chan C.-k., 2008, ApJ, 684, 498
- Ruediger G., Schultz M., Stefani F., Mond M., 2014, ArXiv eprints 1407.0240
- Sano T., Miyama S. M., 1999, ApJ, 515, 776
- Shakura N. I., Sunyaev R. A., 1973, A&A, 24, 337
- Shirakawa K., Hoshino M., 2014, Physics of Plasmas, 21, 052903
- Sorathia K. A., Reynolds C. S., Stone J. M., Beckwith K., 2012, ApJ, 749, 189

Spiegel E. A., Veronis G., 1960, ApJ, 131, 442

Spitzer L., 1962, Physics of Fully Ionized Gases

- Stone J. M., 2011, in IAU Symposium, Vol. 274, IAU Symposium, Bonanno A., de Gouveia Dal Pino E., Kosovichev A. G., eds., pp. 422–428
- Suleimanov V. F., Lipunova G. V., Shakura N. I., 2008, A&A, 491, 267
- Suzuki T. K., Inutsuka S.-i., 2014, ApJ, 784, 121
- Velikhov E. P., 1959, Sov. Phys. JETP, 36, 1398